

ORIGINAL ARTICLE

Acquisition of chromosome 1q duplication in parental and genome-edited human-induced pluripotent stem cell-derived neural stem cells results in their higher proliferation rate in vitro and in vivo

Narges Zare Mehrjardi^{1,2} | Marek Molcanyi¹ | Firuze Fulya Hatay¹ | Marco Timmer³ | Ebrahim Shahbazi² | Justus P. Ackermann⁴ | Stefan Herms^{5,6} | Stefanie Heilmann-Heimbach⁵ | Thomas F. Wunderlich^{4,7,8} | Nora Prochnow⁹ | Aiden Haghikia⁹ | Angelika Lampert¹⁰ | Jürgen Hescheler¹ | Edmund A. M. Neugebauer¹¹ | Hossein Baharvand^{2,12} | Tomo Šarić¹ 

¹Center for Physiology and Pathophysiology, Institute for Neurophysiology, Medical Faculty, University of Cologne, Cologne, Germany

²Department of Stem Cells and Developmental Biology, Cell Science Research Center, Royan Institute for Stem Cell Biology and Technology, ACECR, Tehran, Iran

³Department of Neurosurgery, University Hospital Cologne, Cologne, Germany

⁴Center for Molecular Medicine Cologne, University of Cologne, Cologne, Germany

⁵Department of Genomics, Life & Brain Center, Institute for Human Genetics, University of Bonn, Bonn, Germany

⁶Department of Biomedicine, Medical Genetics, Research Group Genomics, University Hospital Basel, Basel, Switzerland

⁷Max Planck Institute for Metabolism Research and Institute for Genetics, University of Cologne, Cologne, Germany

⁸Cologne Cluster of Excellence in Cellular Stress Responses in Aging-Associated Diseases (CECAD), Cologne, Germany

⁹Clinic for Neurology, St. Josef-Hospital, Clinic of the Ruhr-University Bochum, Bochum, Germany

¹⁰Institute of Physiology, Uniklinik, RWTH Aachen University, Aachen, Germany

¹¹Medizinische Hochschule Brandenburg Theodor Fontane, Campus Neuruppin, Neuruppin, Germany

¹²Department of Developmental Biology, University of Science and Culture, Tehran, Iran

Correspondence

Tomo Šarić, Center for Physiology and Pathophysiology, Institute for Neurophysiology, Medical Faculty, University of Cologne, Robert Koch Str. 39, 50931 Cologne, Germany.
Email: tomo.saric@uni-koeln.de

Present address

Narges Zare Mehrjardi, Department of Preclinical Studies, Clinic for Neurosurgery, University Hospital Düsseldorf, Düsseldorf, Germany

Funding information

Köln Fortune Programm; Deutsche Forschungsgemeinschaft, Grant/Award

Abstract

Objectives: Genetic engineering of human-induced pluripotent stem cell-derived neural stem cells (hiPSC-NSC) may increase the risk of genomic aberrations. Therefore, we asked whether genetic modification of hiPSC-NSCs exacerbates chromosomal abnormalities that may occur during passaging and whether they may cause any functional perturbations in NSCs in vitro and in vivo.

Materials and Methods: The transgenic cassette was inserted into the AAVS1 locus, and the genetic integrity of zinc-finger nuclease (ZFN)-modified hiPSC-NSCs was assessed by the SNP-based karyotyping. The hiPSC-NSC proliferation was assessed in vitro by the EdU incorporation assay and in vivo by staining of brain slices with Ki-67 antibody at 2 and 8 weeks after transplantation of

[Correction added on 26 September 2020, after first online publication: Projekt DEAL funding statement has been added.]

This is an open access article under the terms of the Creative Commons Attribution License, which permits use, distribution and reproduction in any medium, provided the original work is properly cited.

© 2020 The Authors. *Cell Proliferation* Published by John Wiley & Sons Ltd.

Number: SA 1382/7-1 and NE 385/21-1;
Royan Institute

ZFN-NSCs with and without chromosomal aberration into the striatum of immunodeficient rats.

Results: During early passages, no chromosomal abnormalities were detected in unmodified or ZFN-modified hiPSC-NSCs. However, at higher passages both cell populations acquired duplication of the entire long arm of chromosome 1, dup(1)q. ZFN-NSCs carrying dup(1)q exhibited higher proliferation rate than karyotypically intact cells, which was partly mediated by increased expression of *AKT3* located on Chr1q. Compared to karyotypically normal ZFN-NSCs, cells with dup(1)q also exhibited increased proliferation in vivo 2 weeks, but not 2 months, after transplantation.

Conclusions: These results demonstrate that, independently of ZFN-editing, hiPSC-NSCs have a propensity for acquiring dup(1)q and this aberration results in increased proliferation which might compromise downstream hiPSC-NSC applications.

1 | INTRODUCTION

Human-induced pluripotent stem cell-derived neural stem cells (hiPSC-NSCs) have been used for developmental studies,¹ disease modelling,^{2,3} drug screening,⁴ toxicity testing⁵ and in preclinical studies of neuroregenerative therapeutic approaches.⁶ Genetic modification of stem cells is frequently utilized for lineage tracking, to modify the expression of a specific endogenous gene in order to study its biological role, or overexpress exogenous factors to monitor and/or enhance the engraftment and therapeutic efficacy of transplanted cells in regenerative approaches.⁷⁻¹⁰ Genome engineering technologies such as zinc-finger nucleases (ZFN),¹¹ transcription activator-like effector nucleases (TALEN),¹² and the clustered regularly interspaced short palindromic repeats/Cas9 (CRISPR/Cas9) system^{13,14} enable DNA modifications in a highly precise manner and significantly lower the risks of various non-target effects that are associated with traditional genetic engineering techniques.¹⁵ However, genome editing increases cell handling and cultivation time, which could affect their genomic stability and diminish their usefulness because the newly acquired genetic changes may be detrimental to the cell's viability, functionality and safety.¹⁶⁻²⁰

Many studies have demonstrated that different types of stem cells, including NSCs, acquire characteristic chromosomal aberrations during late and sometimes also in early passages in culture.²¹⁻²³ Comprehensive analysis of chromosomal aberrations in 58 adult human NSC samples and 39 human embryonic stem cell (hESC)-derived NSC samples identified a trisomy of chromosomes 7, 10, 19 and 20q as well as a trisomy and monosomy of chromosome 18.²⁴ The overall frequency of aberrations in NSCs was about 9%. A similar frequency of samples with chromosomal aberrations was found in a separate analysis of hiPSC-derived NSCs (10%, 18 out of 182 samples) and adult NSCs (7%, 7 out of 100 samples).²⁵ In these samples, the most common were gains of chromosomes 1, 12 and 17, which also occur in undifferentiated human PSC cultures.^{22,23,26,27}

Targeting safe harbour areas like adeno-associated virus site 1 (AAVS1) by using gene editing methods have been used in various hESC^{11,28} and hiPSC^{9,29} lines and their differentiated derivatives,

such as NSCs.³⁰⁻³² These studies demonstrated that cells modified by genome editing tools exhibited all properties of their parental cells and did not show perturbations in cell viability, proliferation or specialized cell functions. However, it is not fully clear whether gene editing methods increase the frequency of chromosomal aberrations in long-term cultures, whether these aberrations cause any functional perturbations in targeted hiPSC-NSCs and whether these functional changes would still be retained in transplanted cells in vivo.

To address these questions, we used the ZFN technology to integrate a cassette containing a human $\text{EF1-}\alpha$ promoter driving the expression of puromycin resistance gene (Pac) and enhanced GFP (EPG-cassette) into the AAVS1 locus in hiPSC-NSCs. SNP array-based karyotyping identified a duplication of the entire long arm of chromosome 1 [dup(1)q] in unmodified and ZFN-modified NSCs after prolonged passaging. Compared to ZFN-NSCs with an intact karyotype, cells that carried dup(1)q exhibited increased proliferation rate in vitro and in vivo after transplantation into the striatum of immunodeficient rats. The higher proliferation rate was partly mediated by overexpression of the proliferation promoting gene *AKT3* located in duplicated area. These results show that dup(1)q occurs in high-passage hiPSC-NSCs and demonstrate for the first time that its occurrence is not affected by ZFN-based editing but that it increases cell proliferation both in vitro as well as in vivo requiring strict quality control of cells before using them for applications in research and therapy.

2 | MATERIALS AND METHODS

2.1 | ZFN-mediated genome editing

The methods used for construction of the targeting vector pAAVS1-EPG and generation of hiPSC-NSCs are described in the Supplemental material and Figure S1. For transfection, hiPSC-NSCs at passage 14 (p14) were treated overnight with 10 $\mu\text{mol/L}$ ROCK inhibitor (Y-27632, Selleckchem) and then dissociated with 0.05% trypsin-EDTA (Life Technologies). Dissociated hiPSC-NSCs (1×10^6) were re-suspended

in the R buffer from the Neon Transfection System (Life Technologies) together with 8 μg of the pAAVS1-EPG vector and 250 ng of mRNAs encoding ZFNs that target the ZFN cleavage site in the AAVS1 locus and were included in the CompoZr[®] Targeted Integration Kit-AAVS1 (Sigma-Aldrich). Transfection was performed with the Neon Transfection System by using two 20 ms pulses at 1400 V. Transfected cells were plated onto a poly-L-ornithine/laminin-coated (both from Sigma) 6-well plate. Selection with 2 $\mu\text{g}/\text{mL}$ puromycin began at day 7 after transfection. After 10 days, antibiotic-resistant cells were expanded and aliquots were cryopreserved for further studies. The procedures used for generation of single cell clones and identification of mono- and bi-allelic ZFN-NSC lines are described in the Supplemental material, Figure S1, and Tables S1 and S2.

2.2 | Molecular karyotyping

Karyotyping was performed by SNP array-based genotyping using the Human OmniExpressExome-8-v1.2 BeadChip (Illumina, Inc) at the Institute for Human Genetics (Life & Brain Center, University of Bonn, Germany). Processing was performed on gDNA following the manufacturer's procedures. Log R ratio and B-allele frequency plots were generated in GenomeStudio V2011.1 (Illumina, Inc) using the provided manifest and cluster files, version 1.2-B. Copy number regions were detected using the cnvPartition version 3.1.6. A visual inspection was performed for mosaicism states.

2.3 | Cell proliferation assay

Cell proliferation assay was done by Click-iT[®] EdU (5-ethynyl-2'-deoxyuridine) Imaging Kit (Life Technologies). Genetically non-modified wild-type hiPSC-NSCs and gene-edited ZFN-NSCs were plated at the density of $0.1 \times 10^6/\text{cm}^2$ on poly-L-ornithine/laminin-coated plates. Next day, cells were incubated with 10 $\mu\text{mol}/\text{L}$ EdU for 2 hours. After fixation with 3.7% paraformaldehyde and permeabilization with 0.5% Triton X-100, cells were detected with AlexaFluor-555-azide. Stained cells were analysed under Axiovert 200M microscope (Carl-Zeiss) equipped with the image processing software Axiovision 4.5.

2.4 | Protein and gene expression analyses

Immunocytochemical analyses, cDNA synthesis and qPCR amplification of selected genes were carried out as described in the Supplemental material. PCR primers are listed in Table S3 and antibodies in Tables S4 and S5.

2.5 | Transplantation of ZFN-NSCs

Animal experiments were approved by the Landesamt für Natur, Umwelt und Verbraucherschutz NRW, Recklinghausen, Germany

(Permit Number: 84-02.04.2012.A227) and conformed to the Directive 2010/63/EU of the European Parliament. Adult male Rowett Nude rats (RNU; Charles River) that weighed 250-300 g and were 12-14 weeks of age were anaesthetized with intraperitoneal (i.p.) injections of 60 mg/kg body weight pentobarbital. The ZFN-NSC clone 44 without duplication (p14 + 14) and with duplication (p14 + 41) were injected into the striatum of each adult nude rat brain by a Hamilton syringe (5 μL , 33 Gauge, length: 25 mm, Pst4-12; Hamilton) into two injection points with 0.5×10^5 cells/ μL per injection at the following coordinates from the bregma: striatum AP = 0.5, ML = 3.0, DV = -4.5; intraventricular AP = -0.5, ML = 1.2, DV = -3.5. Two weeks and 2 months after NSC transplantation, the animals were sacrificed and transcidentally perfused with 4% paraformaldehyde. Preparation of brain tissue cryosections and immunohistochemistry procedure is described in the Supplemental Material.

2.6 | Statistical analysis

For statistical analysis of differences between experimental groups, the independent two-tailed Student's *t* test was performed by using the GraphPad Prism software (version 4.0). *P* values equal to or lower than .05 were considered statistically significant.

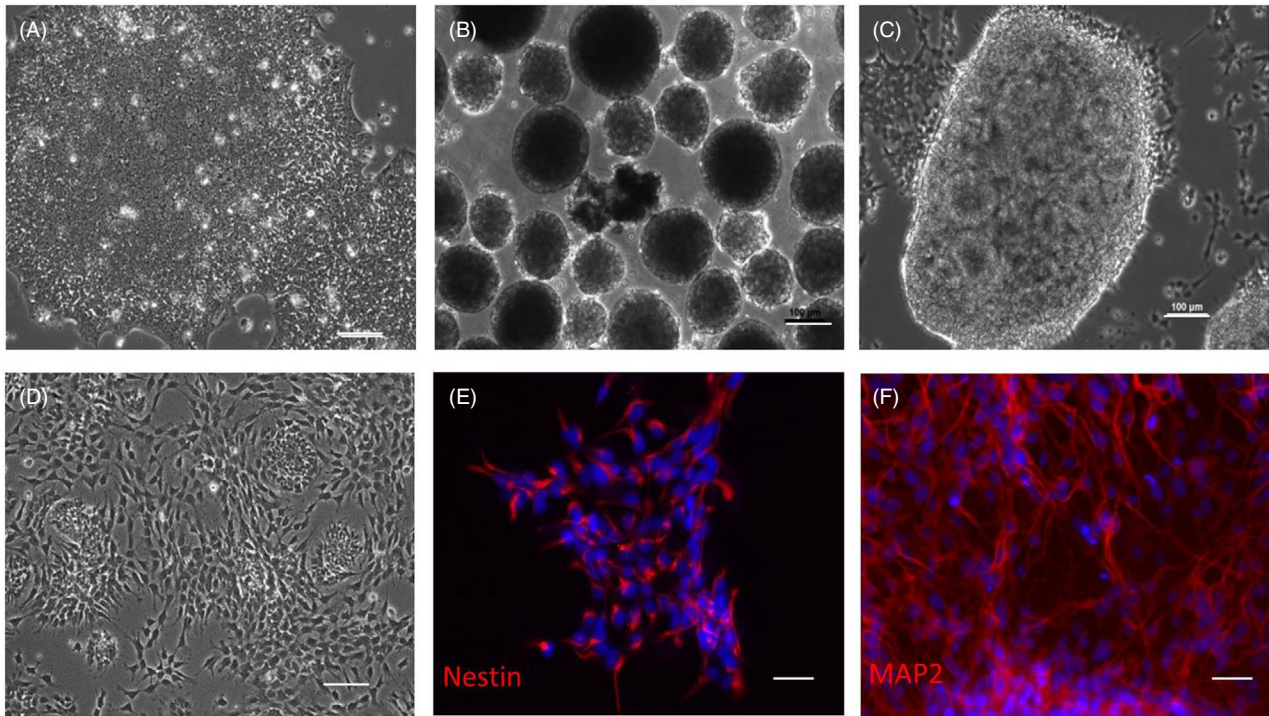
3 | RESULTS

3.1 | Generation and characterization of hiPSC-NSCs

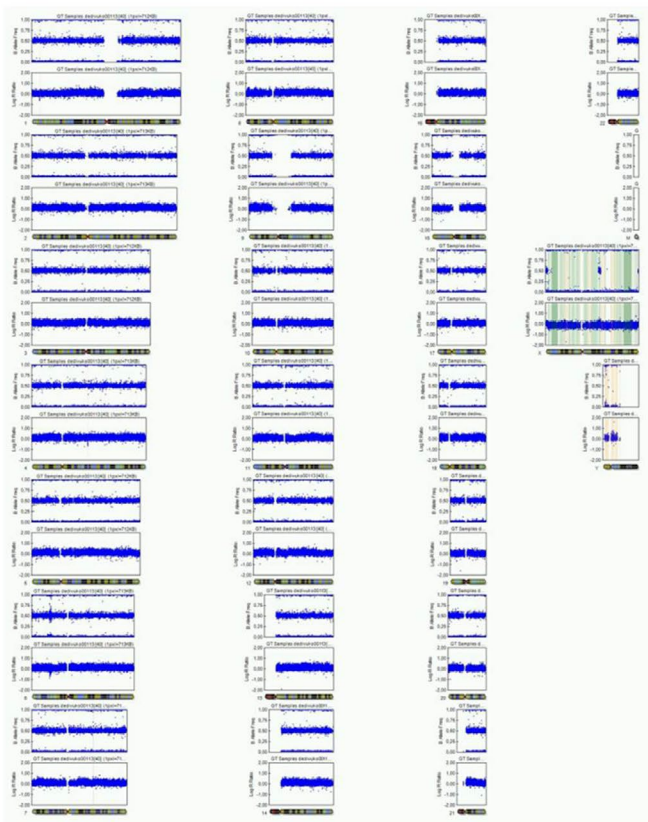
Neural stem cells used in this study were derived from hiPSC line R-iPSC4 as previously reported by us.³³ Transcriptome, proteome and immunocytochemical analyses of these hiPSC-NSCs revealed that they expressed typical NSC markers and exhibited robust differentiation potential to neurons, astrocytes and oligodendrocytes (see reference (33) and Figure 1A-F). Molecular karyotyping of the parental iPSCs at passage 36 (p36) (Figure S2) and of NSCs derived from them at an early time point after their generation (p10) (Figure 1G) showed no structural chromosomal aberrations in these samples. However, after only six additional passages, hiPSC-NSCs acquired a duplication of the entire long arm of chromosome 1 [dup(1)q] but no other abnormalities (Figure 1H, asterisk). This confirms previous reports showing that prolonged maintenance of NSCs in culture leads to the accumulation of lineage-specific gross chromosomal aberrations in a certain fraction of cell lines.^{24,34,35}

3.2 | ZFN-mediated gene targeting into the AAVS1 locus in hiPSC-NSCs

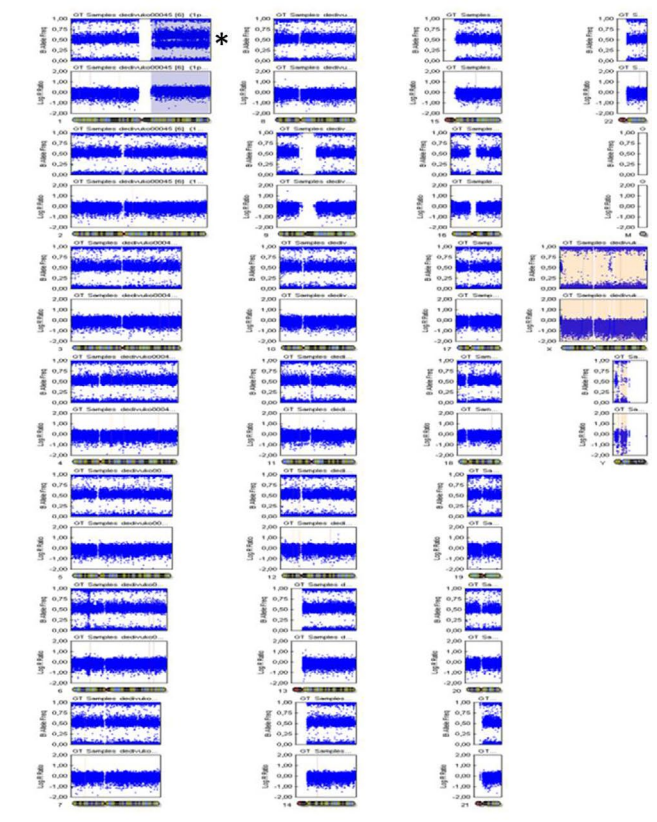
Next, we sought to examine whether ZFN-based genome editing would affect the propensity of hiPSC-NSCs to acquire this or other chromosomal anomalies over prolonged passaging. To this



(G) hiPSC-NSC, p10



(H) hiPSC-NSC, p16



end, the targeting vector pAAVS1-EPG and mRNAs encoding for a pair of ZFNs that target the genomic integration site of AAVS1 locus were co-transfected into R-iPSC4-NSCs at p14. This resulted

in 77% eGFP-positive cells at day two after transfection (Figure S3). Selection with puromycin yielded a pure population of ZFN-edited NSCs that stably expressed eGFP over at least 23 passages in

FIGURE 1 Generation and karyotype analysis of hiPSC-NSCs. A, R-iPSC4-hiPSC colonies growing on Matrigel. B, Embryoid bodies (EBs) formed after digestion of hiPSCs with collagenase IV. C, Rosette-like structures appeared 7-10 d after plating of EBs treated with TGF β -inhibitor SB421543 and BMP-inhibitor dorsomorphin onto poly-L-ornithine- and laminin-coated plates. D, Neuroectodermal cells were obtained by dissociating rosette-like structures and plating on poly-L-ornithine- and laminin-coated plates. E, F, These cells expressed the NSC marker Nestin (E) and differentiated to neurons expressing microtubule-associated protein 2 (MAP2) at day 30 of differentiation (F). Nuclei were stained with Hoechst 33342 (blue). Scale bars: 100 μ m. G, H, Whole-genome SNP array-based karyotyping of hiPSC-NSCs. B-allele frequencies (upper panels) and \log_2 R ratios (lower panels) are plotted for each chromosome for all SNPs on the array located in this region. Each point is an SNP. While cells at passage 10 (p10) did not show any major karyotype abnormalities (G), hiPSC-NSCs at p16 exhibited duplication of the entire long arm of the chromosome 1, dup(1)q (H)

culture (Figure 2A). To obtain homogeneous NSC populations for subsequent studies, we generated clonal ZFN-edited NSC lines by single cell subcloning. After 18 days in culture, single NSCs formed eGFP-positive colonies in 24 out of 192 wells (12.5%). Of these, eight clonal ZFN-NSC lines were established and characterized in more detail. The AAVS1 locus was successfully targeted in seven out of eight ZFN-NSC lines: clone 119 showed no integration at the AAVS1 locus, clone 44 carried the bi-allelic transgene insertion, while clones 124, 128, 138, 164, 183 and 188 carried mono-allelic transgene insertions (Figure 2B; detailed description of these and other related results is provided in Supplemental Results and in Figures S4-S6).

3.3 | Characterization of gene modified hiPSC-NSCs

To determine whether genetic modification and subcloning affected hiPSC-NSCs, we assessed their immunophenotype and differentiation potential. Flow cytometry analysis of the bi-allelic ZFN-NSC clone 44 demonstrated that the expression level of polysialylated neuronal cell adhesion molecule (PSA-NCAM) was comparable to that in parental hiPSC-NSCs (Figure S7A). These cells also retained the ability to form secondary neurospheres (Figure S7B) which could differentiate to microtubule-associated protein 2 (MAP2)-expressing neurons (Figure S7C). Moreover, ZFN-NSCs maintained in monolayer cultures expressed NSC markers Nestin, Sox1 and Pax6, and differentiated towards MAP2- and class III β -tubulin (TUJ1)-expressing neurons, glial fibrillary acidic protein (GFAP)-expressing astrocytes and O4-expressing oligodendrocytes without losing transgenic eGFP expression (Figure 2C and Figure S7D). In addition, electrophysiological analyses showed that neurons derived from parental iPSC-NSCs and both polyclonal and clonal ZFN-NSC lines exhibit comparable functional properties (see Supplemental Results and Figure S8).

3.4 | Molecular karyotyping of ZFN-edited hiPSC-NSCs

Next, we sought to determine which chromosomal aberrations occur in hiPSC-NSCs that underwent the ZFN modification procedure. SNP genotyping of ZFN-NSCs that were kept in culture for

four passages after transfection (p14 + 4) revealed no chromosomal aberrations in these cells (Figure 3A and Figure S9). Chromosomal abnormalities were also not detected after clonal selection of ZFN-NSCs as shown at p14 + 14 for the clone 44 harbouring bi-allelic insertion of the transgene cassette (Figure 3B and Figure S10). However, extended passaging of clonal ZFN-NSCs reproducibly led to the acquisition of a dup(1)q aberration as shown for the bi-allelic clone 44 at p14 + 20 (Figure 3C and Figure S11) and p14 + 36 (Figure 3D and Figure S12), as well as for the mono-allelic clone 138 analysed at p14 + 11 (Figure 3E and Figure S13). Cultivation of clonal ZFN-NSCs for even longer periods of time (p14 + 44) led to the acquisition of additional chromosomal abnormalities, such as duplication of the 10 Mbp large terminal end of the long arm of chromosome 9 (Figure 3F and Figure S14). These results show that dup(1)q is a common aberration both in non-modified as well as ZFN-modified hiPSC-NSCs.

3.5 | Effect of the dup(1)q on the proliferation rate of ZFN-NSCs in vitro

The Chr1q region harbours the genes which are involved in the regulation of cell survival, proliferation and differentiation, such as *AKT3*, *PIK3C2B*, *MDM4* and *NOTCH2NLA*. Therefore, we used the EdU incorporation assay to determine whether dup(1)q affects the proliferation rate of hiPSC-NSCs. This analysis showed that ZFN-mediated genetic modification of NSCs does not affect their proliferative activity in comparison to parental hiPSC-NSCs (Figure 4A,B). However, there was a significantly higher percentage of EdU-positive ZFN-NSCs in cells with dup(1)q compared to those without this aberration ($P < .0001$) (Figure 4C), suggesting that dup(1)q increases the proliferation of hiPSC-NSCs.

Next, we used RT-qPCR analysis to assess whether ZFN-NSCs with and without dup(1)q differ in expression of the above-mentioned genes. These analyses revealed significant upregulation of the *AKT3* (55-fold), *PIK3C2B* (30-fold), *MDM4* (24-fold) and *NOTCH2NLA* (14-fold) transcripts in NSCs carrying dup(1)q compared to their genetically intact counterparts ($n = 3$, $P < .0001$) (Figure 4D). In contrast, expression of *DNMT3B*, which is located on Chr20 and served as a negative control for gene dosage, did not significantly differ between these cell lines. These data show that dup(1)q in NSCs leads to perturbations in expression of genes located on Chr1q and suggest that genes, such as *AKT3* or *PIK3C2B*, might be responsible for their increased proliferation rate.

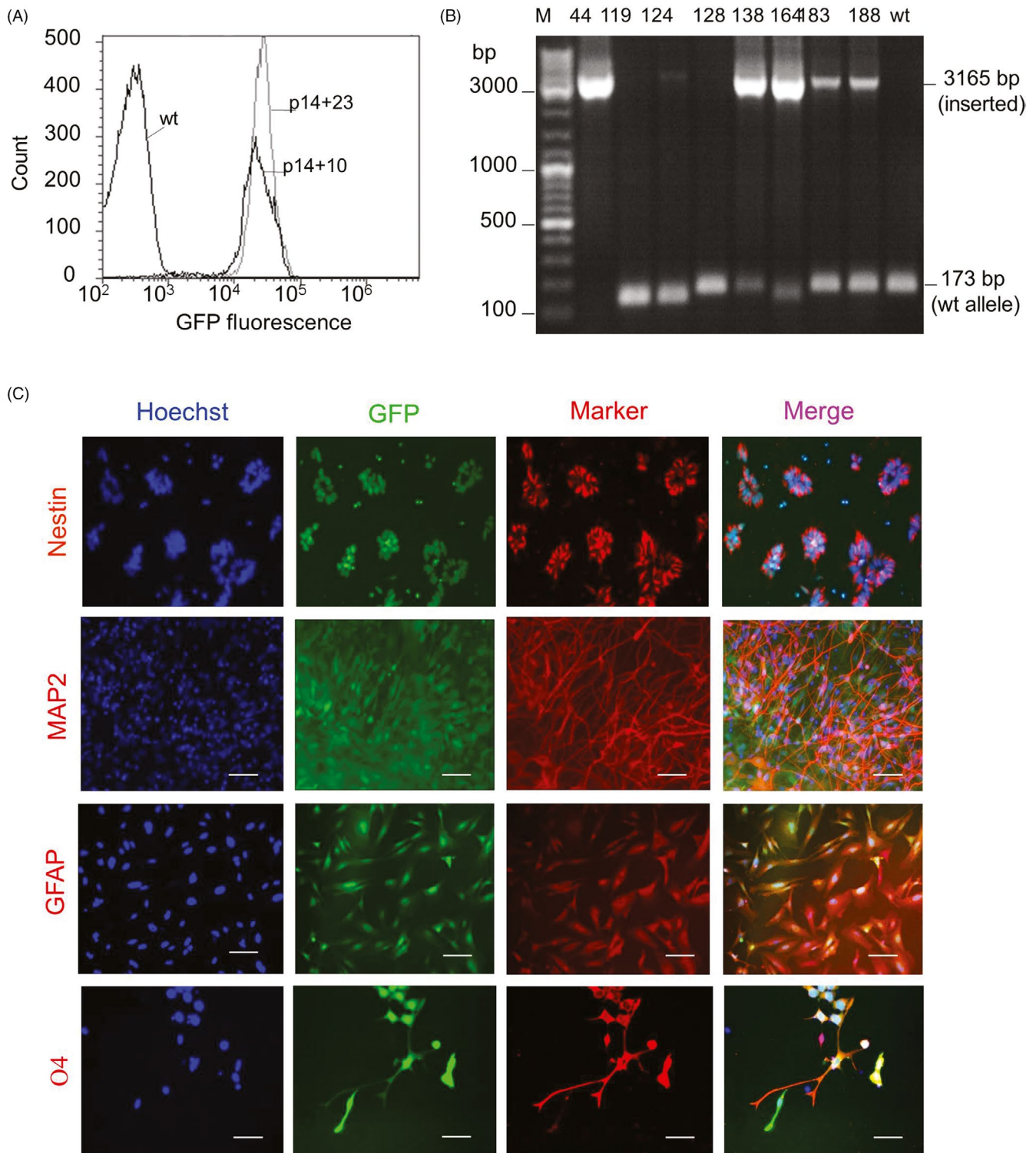


FIGURE 2 Generation and characterization of genetically modified hiPSC-NSCs using zinc-finger nuclease (ZFN) technology. A, Stable expression of eGFP in ZFN-modified hiPSC-NSCs during 13 passages of expansion (from p14 + 10 to p14 + 23) in the absence of puromycin selection. B, Identification of mono- and bi-allelic ZFN-modified hiPSC-NSC-clones by amplification of the genomic DNA (gDNA) with P1 + P2 primers located around the integration site (see Figure S1). Intact AAVS1 locus yielded a PCR product with 173 bp in size while amplicon from the targeted allele has the expected size of 3165 bp. C, Immunostaining of bi-allelic ZFN-NSC clone 44 with antibodies against NSC marker Nestin. Differentiation of ZFN-NSCs to neurons, astrocytes and oligodendrocytes was evaluated by immunocytochemistry using antibodies for microtubule-associated protein 2 (MAP2), glial acidic fibrillary protein (GFAP) and O4, respectively. The expression of transgenic eGFP was retained in all cell lineages. Nuclei were counterstained with Hoechst 33342 (blue). Scale bars: 100 μ m

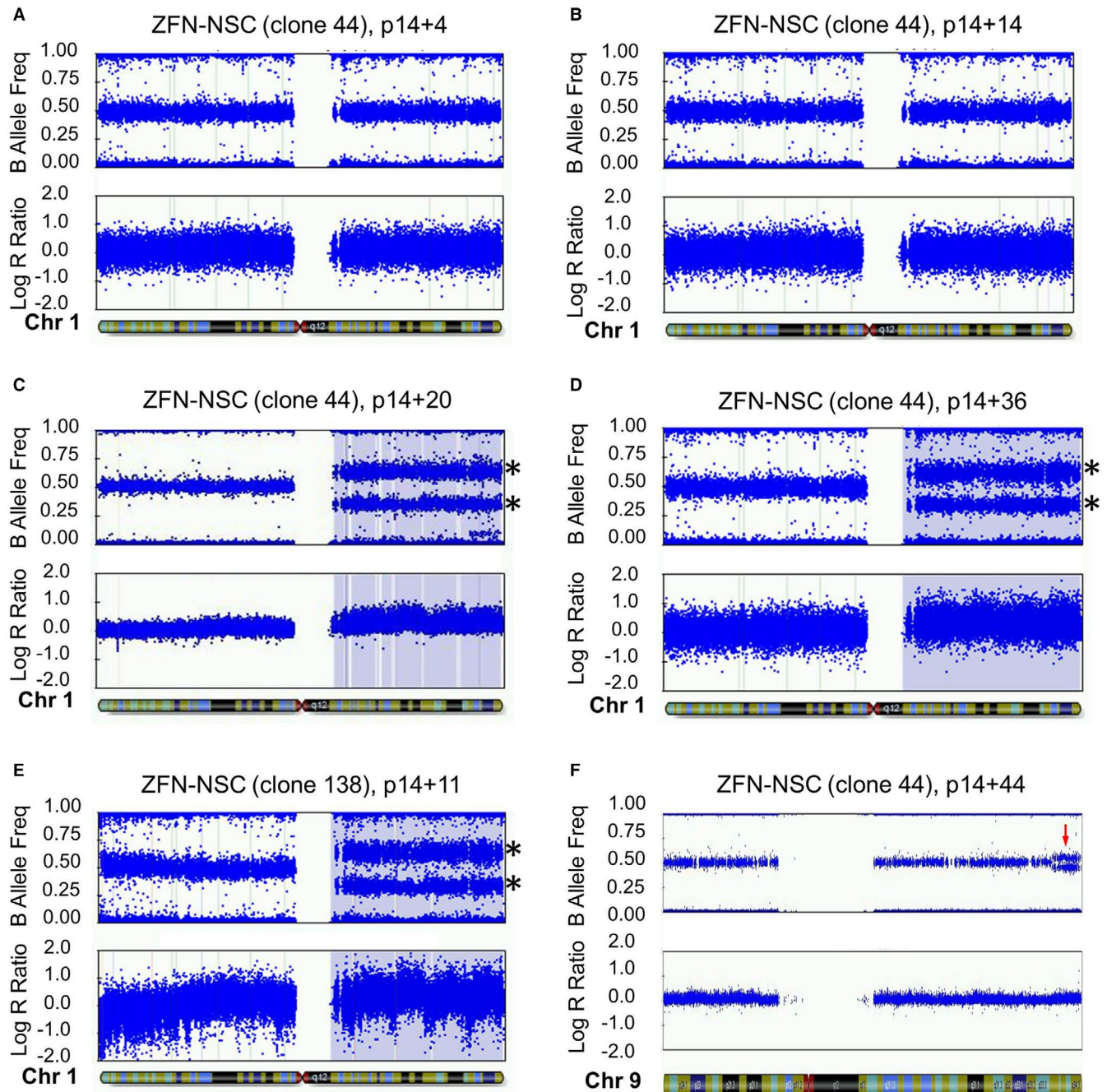
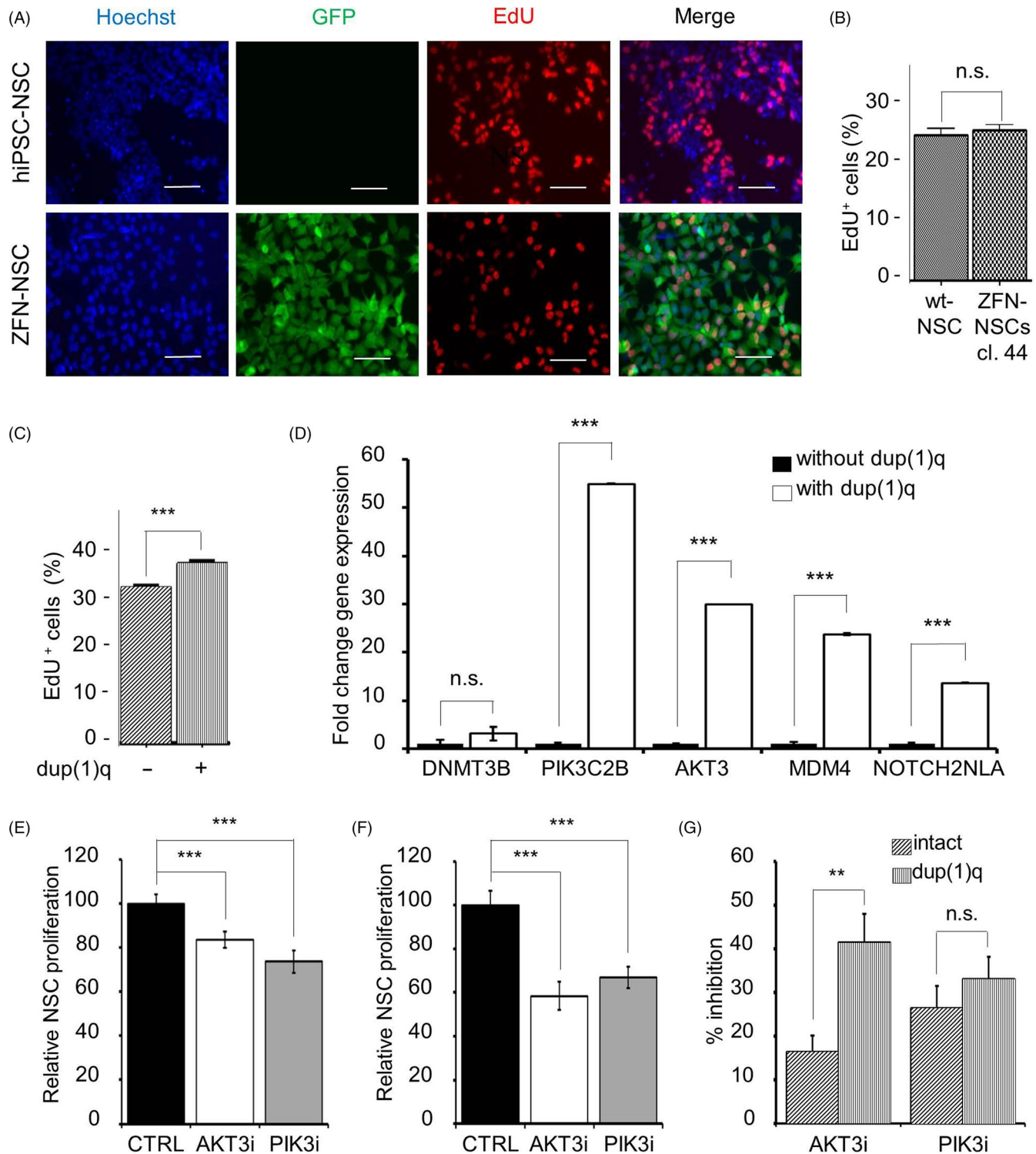


FIGURE 3 SNP array-based karyotyping of different preparations of ZFN-modified hiPSC-NSCs. B-allele frequencies (upper panels) and \log_2 R ratios (lower panels) are plotted for chromosome 1 (A–E) and chromosome 9 (F). The corresponding complete karyotypes are provided in Figures S9–S14. A, Analysis of the heterogeneous population of ZFN-NSCs at p4 after genome modification (p14 + 4) did not reveal any major chromosomal abnormalities (see also Figure S9). B, Early after clonal selection at p14 + 14, the bi-allelic ZFN-NSC clone 44 did not show any detectable aberrations in Chr1 or any other chromosomes (Figure S10). C–E, Extended passaging of clonally selected ZFN-NSCs led to the acquisition of a dup(1)q abnormality (asterisks) as shown for two different batches of clone 44 (batch A at p14 + 20 shown in panel C and Figure S11; batch B at p14 + 36 shown in panel D and Figure S12), and for the mono-allelic clone 138 at p14 + 11 (panel E and Figure S13). F, ZFN-NSC expansion for an even longer period led to the acquisition of additional chromosomal abnormalities as exemplified by the duplication of the 10 Mbp telomeric end in the long arm of chromosome 9 observed in clone 44 at p14 + 44 (arrow see also Figure S14)

3.6 | AKT3 pathway mediates higher proliferation rate of hiPSC-NSCs with dup(1)q

To determine whether AKT3 or PIK3C2B signalling pathways mediate the higher proliferation rate of ZFN-NSCs with dup(1)q, we compared

the EdU incorporation in ZFN-NSCs with and without dup(1)q in the absence and presence of small molecule inhibitors of these protein kinases. This analysis was performed with two independent cell batches, each in triplicate, and reproducibly showed that each inhibitor significantly decreased EdU incorporation both in ZFN-NSCs with and



without dup(1)q (Figure 4E,F). However, the AKT3 inhibitor MK2206 reduced the proliferation of NSCs carrying dup(1)q to a significantly greater extent than the proliferation of karyotypically normal cells (Figure 4G). In contrast, the inhibitory effect of PIK3C2B inhibitor NU7441 did not differ significantly between NSCs with and without dup(1)q (Figure 4G), indicating that AKT3 but not the PIK3C2B signaling pathway at least partly mediates the higher proliferation rate of NSCs with dup(1)q as a consequence of the increased gene dosage.

3.7 | Dup(1)q increases the proliferation rate of ZFN-NSCs in vivo

To determine whether the proliferation-enhancing effect of dup(1)q is also retained in vivo, equal numbers of GFP-expressing ZFN-NSCs (clone 44) with or without this chromosomal aberration were transplanted into the striatum of immunodeficient rat brains ($n = 3$ in each group). Their engraftment and mitotic fractions in the graft

FIGURE 4 Assessment of the proliferation rate and expression of genes located on chromosome 1q in hiPSC-NSCs. A, Fluorescence microscopy of EdU-labelled hiPSC-NSCs (upper panels) and ZFN-NSCs (clone 44, lower panels). Cells were incubated with EdU for 2 h and then stained with EdU antibodies to visualize positive nuclei (red). Only transgenic ZFN-NSCs expressed GFP (green). Nuclei were counterstained with Hoechst 33342 (blue). Scale bars: 100 μ m. B, Quantification of the percentage of EdU-positive NSCs in the experiment shown in panel A based on the scoring of 3087 and 2369 nuclei in non-modified hiPSC-NSCs and ZFN-NSCs (clone 44), respectively (data obtained from two independent experiments, each performed in triplicate). C, The proliferation rate of ZFN-NSCs (clone 44) with (p14 + 44) and without dup(1)q (p14 + 13) as determined by the EdU incorporation assay. The percentage of EdU-positive cells was determined in two independent experiments each performed in triplicate. D, RT-qPCR analysis of *PIK3C2B*, *AKT3*, *MDM4* and *NOTCH2NLA* gene expressions localized on Chr 1q in comparison to *DNMT3B* localized on Chr 20 in ZFN-NSC clone 44 without (p14 + 11) and with dup(1)q (p14 + 41). E,F, ZFN-NSCs (clone 44) without (E) and with dup(1)q (F) were cultured for 24 h in the absence (CTRL) and presence of AKT3 inhibitor (AKT3i) MK2206 or PIK3C2B inhibitor (PIK3i) NU7441 (both at 1 μ mol/L). The proliferation rate was assessed by the EdU incorporation assay as described for panel A. G, Comparison of the extent of inhibition of EdU incorporation into ZFN-NSCs with and without dup(1)q after treatment with AKT3i and PIK3i (calculated from data shown in panels E and F). Treatment with AKT3i, but not PIK3i, exerted a significantly stronger inhibition on the proliferation rate of ZFN-NSCs with dup(1)q than on genetically intact ZFN-NSCs. n.s.: Non-significant, ** $P < .01$ and *** $P < .001$

area were analysed 2 weeks and 2 months after transplantation. The 2-week analysis of brain slices revealed that transplanted ZFN-NSCs in both groups formed well-delineated grafts which expressed GFP as well as the human-specific marker TRA-1-85 (Figure 5A,E). Immunohistochemistry revealed that most injected cells in both groups expressed this NSC marker Nestin (Figure 5B,F), indicating that at this early time point after transplantation they had not differentiated into neural cell lineages. Assessment of the proliferative activity within the graft area by using an antibody against the proliferation marker Ki-67 showed that $38 \pm 8\%$ of NSCs with dup(1)q were Ki-67 positive, while only $11 \pm 15\%$ of NSCs without duplication expressed this marker ($P < .05$, Figure 5C,D,G-I).

At 2 months after transplantation, some immature Nestin-positive ZFN-NSCs still persisted in the brain (Figure S15A,E) but most ZFN-NSCs appeared to have differentiated into MAP2-expressing neurons that overlapped with the human nuclear antigen (HNA) signal in both experimental groups (Figure S15B,F). Confocal microscopy of the section of rat brain transplanted with ZFN-NSCs carrying dup(1)q revealed that MAP2- and HNA-positive cells projected their neurites into the striatum, which confirmed maturation of ZFN-NSC-derived neurons and integration into the brain tissue (Figure S16A,B). Ki-67 staining revealed that only $0.52 \pm 0.52\%$ of NSCs without the duplication and $3.31 \pm 2.28\%$ of cells with dup(1)q were mitotically active (Figure S15C,D,G-I), but this difference was not statistically significant ($P > .05$). These data demonstrate that the pro-proliferative effect of dup(1)q in hiPSC-NSCs also persists in vivo and that it is most pronounced in the first few weeks after transplantation before NSCs differentiate to neural cells.

4 | DISCUSSION

NSCs derived from human ESCs and iPSCs are important vehicles for genetic and molecular therapies in the central nervous system. Genetic modifications of these cells allow for monitoring their differentiation progress,³⁶ improve our understanding of neural development and disease,³⁷ and may increase their potential for regenerative

therapies.³⁸ To overcome the disadvantages of genetic modification methods based on random integration, we used ZFN technology for targeted genome modification in hiPSC-NSCs. Most genome editing studies in the past several years have employed the CRISPR/Cas9 technology because this technology is much more simple, affordable and efficient than ZFN- and TALEN-based systems for targeting any desired single or multiple genomic loci.¹⁴ However, for introduction of a defined expression cassette into a single genomic safe harbour locus pre-designed ZFN- or TALEN-reagents can be equally useful. By using the ZFN-nuclease commercial kit, we showed that integration of the expression cassette into the AAVS1 locus in hiPSC-NSCs is highly efficient, enables stable long-term transgene expression and does not adversely affect the NSC characteristics both before as well as after single cell cloning. This is in agreement with previous studies in ZFN-modified human foetal NSCs,³¹ TALEN-modified hiPSC-NSCs³⁰ and CRISPR/Cas9-targeted human^{7,32} and mouse brain-derived NSCs.^{32,39} However, the chromosomal integrity and functional consequences that chromosomal aberrations might induce in gene targeted NSCs in vitro and in vivo have not been addressed in these previous studies. Here, we show that prolonged culture of hiPSC-NSCs leads to the acquisition of dup(1)q independently of whether they were genetically modified by ZFNs or not, and that this aberration increases NSC proliferation in vitro as well as in vivo in the first weeks after transplantation most likely by activation of the AKT3 signalling pathway.

The mechanism responsible for occurrence of dup(1)q in hiPSC-NSCs is not known. In the literature, several mechanisms have been implicated in the acquisition of genomic instability and aneuploidy in hPSCs. For example, Lamm and coworkers have shown that decreased expression of the transcription factor SRF, which controls the activity of actin cytoskeletal genes, induces replicative stress and chromosomal condensation defects that underlie the ongoing chromosomal instability seen in aneuploid hPSCs.⁴⁰ They suggested that similar mechanism may also operate during initiation of chromosomal instability in diploid hPSCs. In addition, Zhang and coworkers reported that loss-of-function mutations in pro-apoptotic genes or upregulation of anti-apoptotic genes that may occur in hPSC desensitize them to mitotic stress and enable aneuploid cell survival.⁴¹

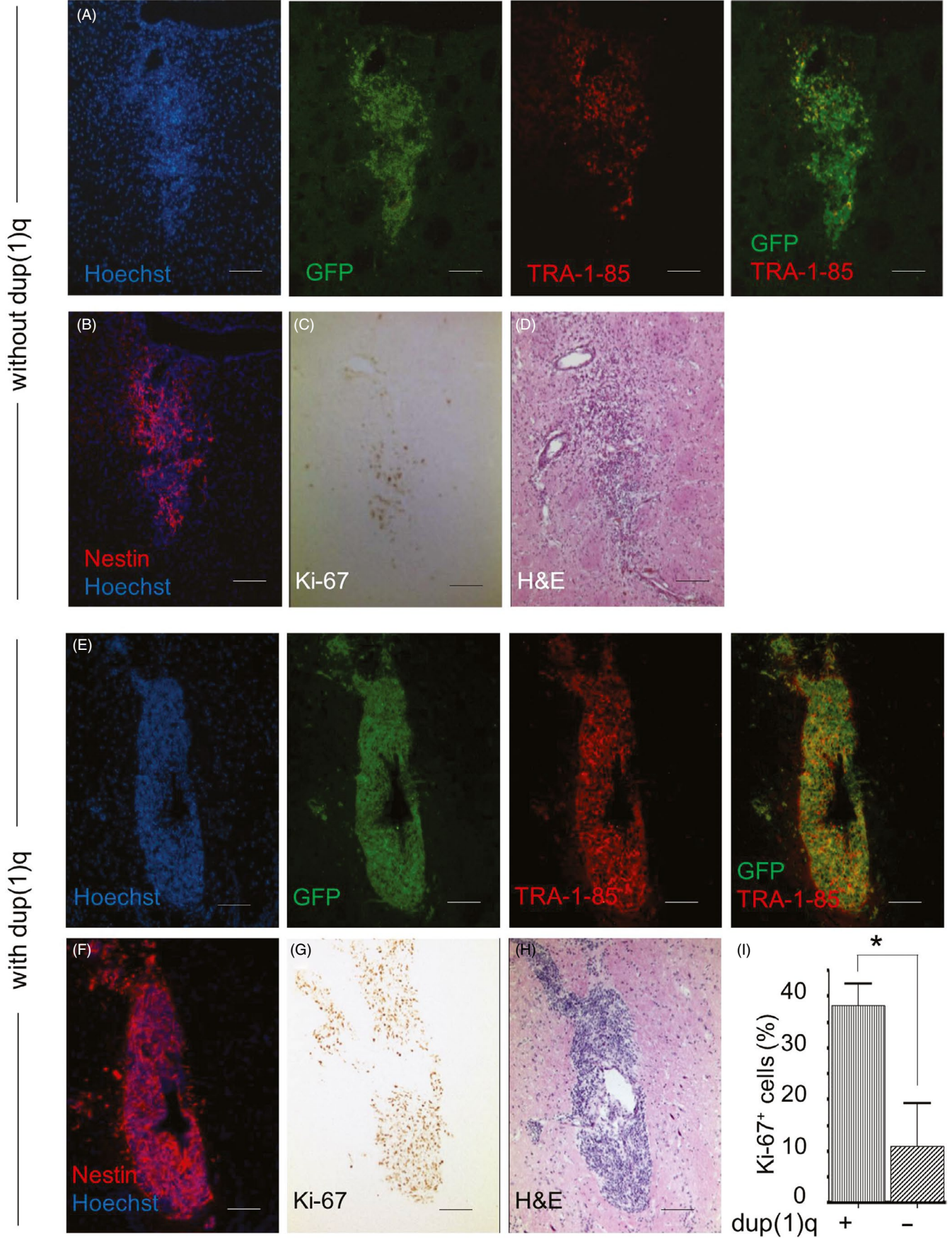


FIGURE 5 In vivo engraftment and proliferation rate of ZFN-NSCs with and without dup(1)q. A, E, Representative images of brain slices stained with antibodies against transgenic eGFP and human cell marker TRA-1-85 2 weeks after transplantation of ZFN-NSCs (clone 44) without dup(1)q (A) and with dup(1)q (E) into the striatum of RNU rats. B, F, Expression of Nestin (red) in engrafted ZFN-NSCs indicates that, independently of karyotype status, most transplanted cells had not differentiated to neural cells. C, G, Mitotic NSCs in the graft area were detected by staining for the proliferation marker Ki-67 and counterstaining with haematoxylin and eosin (D,H). I, The percentage of Ki-67-positive ZFN-NSCs was significantly higher in engrafted dup(1)q cells than in grafts containing karyotypically normal NSCs. The total number of nuclei counted in animals transplanted with NSCs with and without dup(1)q was 2991 and 452, respectively. Hoechst 33342 was used to label the nuclei (blue). * $P < .05$. Scale bars: 100 μ m

Other studies identified POLD3 and ZSCAN10 as factors involved in maintenance of genomic stability in PSCs. POLD3 is a gene encoding for the accessory subunit of DNA polymerase delta 3, and its loss results in replicative stress, DNA repair impairment, micronucleation and aneuploidy in ESCs.⁴² The embryonic stem cell-specific transcription factor ZSCAN10 has been shown to protect hPSCs from accumulation of chromosomal structural abnormalities, and defects in apoptosis and in the DNA damage response.⁴³ The mechanism which is specifically responsible for the acquisition of dup(1)q in hiPSC-NSCs will be explored in future studies.

Gains of chromosome 1 have been detected by other groups both in NSCs^{25,44} as well as in human ESCs and iPSCs.^{22,23,27,45} Among them were whole chromosome 1 duplications (trisomy) or unbalanced translocations and interstitial duplications of different segments in its long arm. For example, Weissbein and coworkers observed duplication of the whole chromosome 1q in human PSC-NSCs but they did not assess its functional consequences.²⁵ In contrast, Varela and coworkers detected amplification of a segment of 1q and its translocation onto the telomeric ends of chromosomes 5p, 8q and 13q in long-term cultured hESC-NSCs.⁴⁴ They also showed that neuronal differentiation of two aberrant NSC lines was decreased in vitro but this was not systematically observed in all lines that were tested. In addition, ESC-NSCs carrying the unbalanced 1q translocation failed to integrate into the striatum of the rat brain at 7 weeks after transplantation. Although the study by Varela et al suggested that the duplication of a 1q segment or its translocation onto different recipient chromosomes could hamper the NSC differentiation in vitro and survival in vivo, this effect was not observed in our hiPSC-NSCs with dup(1)q. The most likely reason for this is in the different nature of duplication identified in our studies.

It is worth noting that the human chromosome 1q corresponds to mouse chromosomes 1 and 3. Interestingly, gain of the entire chromosome 1 was observed in long-term cultured NSCs derived from mouse ESCs or adult and foetal mouse brain.^{46,47} In the study with mouse foetal brain-derived NSCs, cells carrying trisomy 1 exhibited increased proliferation and decreased neural differentiation capacity in vitro.⁴⁷ Aberrations in 1q are also one of the most common abnormalities reported among human neoplasms, including haematologic malignancies⁴⁸⁻⁵⁰ and paediatric brain tumours,⁵¹⁻⁵³ suggesting that they might be associated with advantages in cell proliferation and survival. Indeed, the proliferation rate of hiPSC-NSCs carrying dup(1)q in our study was higher than that of karyotypically normal NSCs both in vitro and in vivo. The identification of specific driver gene(s) on chromosome 1q responsible for this effect in NSCs or cancer cells is difficult because

more than one gene could be involved in conveying the growth advantage to aneuploid cells. However, number of genes located on chromosome 1q, such as *AKT3*, *PIK3C2B*, *MDM4* and *NOTCH2NL*, are known to be associated with the control of cell proliferation, survival, migration, stress response, oncogenic transformation, neuronal differentiation and intracellular protein trafficking.⁵⁴⁻⁵⁷ Interestingly, these genes were found to be overexpressed in ZFN-NSCs with dup(1)q and inhibitor studies suggested that *AKT3* pathway may be at least partially responsible for their increased proliferation rate.

Contrary to the observation by Varela and coworkers that hESC-NSCs carrying chromosomal 1q duplication exhibit altered in vitro differentiation and in vivo engraftment,⁴⁴ the dup(1)q aberration in our study did not affect the integration of ZFN-NSCs into the rat striatum and 2 weeks after transplantation they still showed enhanced proliferation compared to NSCs without duplication. At this time point, most transplanted cells expressed Nestin and did not exhibit any detectable neuronal cell differentiation, which explains the high proliferation rate observed at this time point. After 2 months, the cells with duplication also exhibited more than a three-fold higher fraction of dividing cells than control cells. However, the overall number of Ki-67-positive cells was very low and not significantly different between control and mutant cell populations. Although we could still detect Nestin-positive ZFN-NSCs in the graft area at this time point, many transplanted NSCs differentiated into neurons which appeared to make synaptic connections to neighbouring areas, indicating their functional integration into the host tissue. We observed no tumour formation after 2 months of transplantation, but we cannot exclude the tumorigenicity of cells carrying duplication after a longer period. This should be explored in future studies because this adverse effect occurred 4 years after transplantation of foetal NSCs in a patient with ataxia telangiectasia.⁵⁸

In conclusion, we show that an isolated duplication of chromosome 1q occurs in unmodified and ZFN-modified hiPSC-NSCs after prolonged passaging, that this aberration increases NSC proliferation rate in vitro, and that these changes still persist in transplanted cells in vivo. Our preliminary data suggest that the higher proliferation rate of aberrant NSCs is partly mediated by overexpression of the proliferation promoting gene *AKT3* located in duplicated area, but additional studies are required to elucidate the exact mechanism responsible for this phenomenon. It should be noted that in some prior studies no chromosomal abnormalities were observed in the long-term cultured hPSC-NSCs.^{59,60} This indicates that acquisition of such abnormalities in cultured cells is not an inevitable event and that conditions might be selected that

prevent their occurrence as it was demonstrated in several previous studies.^{43,61-65} Nevertheless, the genomic integrity of all cell products used for regenerative approaches should be carefully assessed and monitored to ensure that they are safe and therapeutically effective.

ACKNOWLEDGMENTS

This project was supported by funds from the Deutsche Forschungsgemeinschaft (DFG) to T.Š. and EN (grant numbers: SA 1382/7-1 and NE 385/21-1), by the Köln Fortune Programm to T.Š. and from Royan institute to HB We thank Karina Neumann, Rebecca Dieterich and the staff of the Animal Facility Network of the Medical Faculty of the University of Cologne for technical assistance. None of the authors declared a financial conflict of interest related to the submitted manuscript.

Open access funding enabled and organized by Projekt DEAL

CONFLICT OF INTEREST

None of the authors have a conflict of interest to declare. None of the three authors affiliated with the Royan Institute (NZM, ES and HB) are employed by a government agency that has a primary function other than research and/or education, and they are not submitting this manuscript as an official representative or on behalf of their government. This study was entirely performed at the University of Cologne in Germany and was funded by the German Research Foundation (DFG). Results described in this manuscript were used by Narges Zare Mehrjardi in partial fulfilment of the requirements for her PhD degree at the University of Cologne without involvement of any government agency.

AUTHOR CONTRIBUTIONS

Investigation, formal analysis, validation and writing of the original draft: NZM; investigation, methodology, formal analysis, validation and supervision: MM, AH and AL; investigation and formal analysis: FFH, ES, JPA, SH and NP; resources: MT, JH, SHH and TFW; resources, writing—review and editing: HB; conceptualization and funding acquisition: EAMN; conceptualization, funding acquisition, project administration, supervision, writing—original draft, review and editing: T.Š. All authors have read and approved the final version of the manuscript.

DATA AVAILABILITY STATEMENT

The data that support the findings of this study are available from the corresponding author upon reasonable request.

ORCID

Tomo Šarić  <https://orcid.org/0000-0001-8344-1095>

REFERENCES

- Suzuki IK, Vanderhaeghen P. Is this a brain which I see before me? Modeling human neural development with pluripotent stem cells. *Development*. 2015;142:3138-3150.
- Engle SJ, Blaha L, Kleiman RJ. Best practices for translational disease modeling using human iPSC-derived neurons. *Neuron*. 2018;100:783-797.
- Hollingsworth EW, Vaughn JE, Orack JC, et al. iPheMap: an atlas of phenotype to genotype relationships of human iPSC models of neurological diseases. *EMBO Mol Med*. 2017;9:1742-1762.
- Farkhondeh A, Li R, Gorshkov K, et al. Induced pluripotent stem cells for neural drug discovery. *Drug Discov Today*. 2019;24:992-999.
- Liang SX, Yin NY, Faiola F. Human pluripotent stem cells as tools for predicting developmental neural toxicity of chemicals: strategies, applications, and challenges. *Stem Cells Dev*. 2019;28:755-768.
- Takahashi J. Stem cells and regenerative medicine for neural repair. *Curr Opin Biotechnol*. 2018;52:102-108.
- Dever DP, Scharenberg SG, Camarena J, et al. CRISPR/Cas9 genome engineering in engraftable human brain-derived neural. *Stem Cells*. 2019;15:524-535.
- Wang Y, Zhang WY, Hu S, et al. Genome editing of human embryonic stem cells and induced pluripotent stem cells with zinc finger nucleases for cellular imaging. *Circ Res*. 2012;111:1494-1503.
- Luo Y, Liu C, Cerbini T, et al. Stable enhanced green fluorescent protein expression after differentiation and transplantation of reporter human induced pluripotent stem cells generated by AAVS1 transcription activator-like effector nucleases. *Stem Cells Transl Med*. 2014;3:821-835.
- Fu X, Rong Z, Zhu S, Wang X, Xu Y, Lake BB. Genetic approach to track neural cell fate decisions using human embryonic stem cells. *Protein Cell*. 2014;5:69-79.
- Hockemeyer D, Soldner F, Beard C, et al. Efficient targeting of expressed and silent genes in human ESCs and iPSCs using zinc-finger nucleases. *Nat Biotechnol*. 2009;27:851-857.
- Ding Q, Lee YK, Schaefer EA, et al. A TALEN genome-editing system for generating human stem cell-based disease models. *Cell Stem Cell*. 2013;12:238-251.
- Ben Jehuda R, Shemer Y, Binah O. Genome editing in induced pluripotent stem cells using CRISPR/Cas9. *Stem Cell Rev Rep*. 2018;14:323-336.
- Zhang Z, Zhang Y, Gao F, et al. CRISPR/Cas9 genome-editing system in human stem cells: current status and future prospects. *Mol Ther Nucleic Acids*. 2017;9:230-241.
- Veres A, Gosis BS, Ding Q, et al. Low incidence of off-target mutations in individual CRISPR-Cas9 and TALEN targeted human stem cell clones detected by whole-genome sequencing. *Cell Stem Cell*. 2014;15:27-30.
- Ben-David U, Arad G, Weissbein U, et al. Aneuploidy induces profound changes in gene expression, proliferation and tumorigenicity of human pluripotent stem cells. *Nat Commun*. 2014;5:4825.
- Markouli C, De Deckersberg EC, Regin M, et al. Gain of 20q11.21 in human pluripotent stem cells impairs TGF-beta-dependent neuroectodermal commitment. *Stem Cell Reports*. 2019;13:163-176.
- Newman DL, Thurgood LA, Gregory SL. The impact of aneuploidy on cellular homeostasis. *Free Radic Res*. 2019;53:705-713.
- Henry MP, Hawkins JR, Boyle J, Bridger JM. The genomic health of human pluripotent stem cells: genomic instability and the consequences on nuclear organization. *Front Genet*. 2018;9:623.
- Nguyen HT, Geens M, Mertzanidou A, et al. Gain of 20q11.21 in human embryonic stem cells improves cell survival by increased expression of Bcl-xL. *Mol Hum Reprod*. 2014;20:168-177.
- Na J, Baker D, Zhang J, Andrews PW, Barbaric I. Aneuploidy in pluripotent stem cells and implications for cancerous transformation. *Protein Cell*. 2014;5:569-579.
- Mayshar Y, Ben-David U, Lavon N, et al. Identification and classification of chromosomal aberrations in human induced pluripotent stem cells. *Cell Stem Cell*. 2010;7:521-531.
- Amps K, Andrews PW, Anyfantis G, et al. Screening ethnically diverse human embryonic stem cells identifies a chromosome 20 minimal amplicon conferring growth advantage. *Nat Biotechnol*. 2011;29:1132-1144.

24. Ben-David U, Mayshar Y, Benvenisty N. Large-scale analysis reveals acquisition of lineage-specific chromosomal aberrations in human adult stem cells. *Cell Stem Cell*. 2011;9:97-102.
25. Weissbein U, Ben-David U, Benvenisty N. Virtual karyotyping reveals greater chromosomal stability in neural cells derived by transdifferentiation than those from stem cells. *Cell Stem Cell*. 2014;15:687-691.
26. Draper JS, Smith K, Gokhale P, et al. Recurrent gain of chromosomes 17q and 12 in cultured human embryonic stem cells. *Nat Biotechnol*. 2004;22:53-54.
27. Baker DE, Harrison NJ, Maltby E, et al. Adaptation to culture of human embryonic stem cells and oncogenesis in vivo. *Nat Biotechnol*. 2007;25:207-215.
28. Liu Z, Wang Z, Li Y, et al. Association of genomic instability, and the methylation status of imprinted genes and mismatch-repair genes, with neural tube defects. *Eur J Hum Genet*. 2012;20:516-520.
29. Hockemeyer D, Wang H, Kiani S, et al. Genetic engineering of human pluripotent cells using TALE nucleases. *Nat Biotechnol*. 2011;29:731-734.
30. Cerbini T, Funahashi R, Luo Y, et al. Transcription activator-like effector nuclease (TALEN)-mediated CLYBL targeting enables enhanced transgene expression and one-step generation of dual reporter human induced pluripotent stem cell (iPSC) and neural stem cell (NSC) lines. *PLoS One*. 2015;10:e0116032.
31. Lombardo A, Cesana D, Genovese P, et al. Site-specific integration and tailoring of cassette design for sustainable gene transfer. *Nat Methods*. 2011;8:861-869.
32. Bressan RB, Dewari PS, Kalantzaki M, et al. Efficient CRISPR/Cas9-assisted gene targeting enables rapid and precise genetic manipulation of mammalian neural stem cells. *Development*. 2017;144:635-648.
33. Simao D, Silva MM, Terrasso AP, et al. Recapitulation of human neural microenvironment signatures in iPSC-derived NPC 3D differentiation. *Stem Cell Reports*. 2018;11:552-564.
34. Murrell W, Palmero E, Bianco J, et al. Expansion of multipotent stem cells from the adult human brain. *PLoS One*. 2013;8:e71334.
35. Sareen D, McMillan E, Ebert AD, et al. Chromosome 7 and 19 trisomy in cultured human neural progenitor cells. *PLoS One*. 2009;4:e7630.
36. Zhang Y, Zhang Z, Chen P, et al. Directed differentiation of notochord-like and nucleus pulposus-like cells using human pluripotent stem cells. *Cell Rep*. 2020;30(8):2791-2806.e5.
37. Paquet D, Kwart D, Chen A, et al. Efficient introduction of specific homozygous and heterozygous mutations using CRISPR/Cas9. *Nature*. 2016;533:125-129.
38. Poppe D, Doerr J, Schneider M, et al. Genome editing in neuroepithelial stem cells to generate human neurons with high adenosine-releasing capacity. *Stem Cells Transl Med*. 2018;7:477-486.
39. Dewari PS, Southgate B, McCarten K, et al. An efficient and scalable pipeline for epitope tagging in mammalian stem cells using Cas9 ribonucleoprotein. *eLife*. 2018;7.
40. Lamm N, Ben-David U, Golan-Lev T, Storchova Z, Benvenisty N, Kerem B. Genomic instability in human pluripotent stem cells arises from replicative stress and chromosome condensation defects. *Cell Stem Cell*. 2016;18:253-261.
41. Zhang J, Hirst AJ, Duan F, et al. Anti-apoptotic mutations desensitize human pluripotent stem cells to mitotic stress and enable aneuploid cell survival. *Stem Cell Reports*. 2019;12:557-571.
42. Zhou ZC, Wang LL, Ge FX, et al. Pold3 is required for genomic stability and telomere integrity in embryonic stem cells and meiosis. *Nucleic Acids Res*. 2018;46:3468-3486.
43. Skamagki M, Correia C, Yeung P, et al. ZSCAN10 expression corrects the genomic instability of iPSCs from aged donors. *Nat Cell Biol*. 2017;19:1037-1048.
44. Varela C, Denis JA, Polentes J, et al. Recurrent genomic instability of chromosome 1q in neural derivatives of human embryonic stem cells. *J Clin Invest*. 2012;122:569-574.
45. Dekel-Naftali M, Aviram-Goldring A, Litmanovitch T, et al. Screening of human pluripotent stem cells using CGH and FISH reveals low-grade mosaic aneuploidy and a recurrent amplification of chromosome 1q. *Eur J Hum Genet*. 2012;20:1248-1255.
46. Diaferia GR, Conti L, Redaelli S, et al. Systematic chromosomal analysis of cultured mouse neural stem cell lines. *Stem Cells Dev*. 2011;20:1411-1423.
47. Vukicevic V, Jauch A, Dinger TC, et al. Genetic instability and diminished differentiation capacity in long-term cultured mouse neurosphere cells. *Mech Ageing Dev*. 2010;131:124-132.
48. Oshimura M, Sonta S, Sandberg AA. Trisomy of the long arm of chromosome No. 1 in human leukemia. *J Natl Cancer Inst*. 1976;56:183-184.
49. Knuutila S, Bjorkqvist AM, Autio K, et al. DNA copy number amplifications in human neoplasms: review of comparative genomic hybridization studies. *Am J Pathol*. 1998;152:1107-1123.
50. Sawyer JR, Tricot G, Mattox S, Jagannath S, Barlogie B. Jumping translocations of chromosome 1q in multiple myeloma: evidence for a mechanism involving decondensation of pericentromeric heterochromatin. *Blood*. 1998;91:1732-1741.
51. Gilbert F, Feder M, Balaban G, et al. Human neuroblastomas and abnormalities of chromosomes 1 and 17. *Cancer Res*. 1984;44:5444-5449.
52. Combaret V, Turc-Carel C, Thiesse P, et al. Sensitive detection of numerical and structural aberrations of chromosome 1 in neuroblastoma by interphase fluorescence in situ hybridization. Comparison with restriction fragment length polymorphism and conventional cytogenetic analyses. *Int J Cancer*. 1995;61:185-191.
53. Manotham K, Chattong S, Setpakdee A. Generation of CCR5-defective CD34 cells from ZFN-driven stop codon-integrated mesenchymal stem cell clones. *J Biomed Sci*. 2015;22:25.
54. Fiddes IT, Lodewijk GA, Mooring M, et al. Human-specific NOTCH2NL genes affect notch signaling and cortical neurogenesis. *Cell*. 2018;173(6):1356-1369.e22.
55. Haupt S, Mejia-Hernandez JO, Vijayakumaran R, Keam SP, Haupt Y. The long and the short of it: the MDM4 tail so far. *J Mol Cell Biol*. 2019;11:231-244.
56. Lopes F, Torres F, Soares G, et al. The role of AKT3 copy number changes in brain abnormalities and neurodevelopmental disorders: four new cases and literature review. *Front Genet*. 2019;10:58.
57. Ping Y, Deng Y, Wang L, et al. Identifying core gene modules in glioblastoma based on multilayer factor-mediated dysfunctional regulatory networks through integrating multi-dimensional genomic data. *Nucleic Acids Res*. 2015;43:1997-2007.
58. Amariglio N, Hirshberg A, Scheithauer BW, et al. Donor-derived brain tumor following neural stem cell transplantation in an ataxia telangiectasia patient. *PLoS Medicine*. 2009;6:e1000029.
59. Koch P, Opitz T, Steinbeck JA, Ladewig J, Brustle O. A rosette-type, self-renewing human ES cell-derived neural stem cell with potential for in vitro instruction and synaptic integration. *Proc Natl Acad Sci USA*. 2009;106:3225-3230.
60. Nemati S, Hatami M, Kiani S, et al. Long-term self-renewable feeder-free human induced pluripotent stem cell-derived neural progenitors. *Stem Cells Dev*. 2011;20:503-514.
61. Thompson O, von Meyenn F, Hewitt Z, et al. Low rates of mutation in clinical grade human pluripotent stem cells under different culture conditions. *Nat Commun*. 2020;11:1528.
62. Jacobs K, Zambelli F, Mertzanidou A, et al. Higher-density culture in human embryonic stem cells results in DNA damage and genome instability. *Stem Cell Reports*. 2016;6:330-341.
63. Prakash Bangalore M, Adhikarla S, Mukherjee O, Panicker MM. Genotoxic effects of culture media on human pluripotent stem cells. *Sci Rep*. 2017;7:42222.
64. Halliwell JA, Frith TJR, Laing O, et al. Nucleosides rescue replication-mediated genome instability of human pluripotent stem cells. *Stem Cell Reports*. 2020;14:1009-1017.

65. Guo R, Ye X, Yang J, et al. Feeders facilitate telomere maintenance and chromosomal stability of embryonic stem cells. *Nat Commun.* 2018;9:2620.

SUPPORTING INFORMATION

Additional supporting information may be found online in the Supporting Information section.

How to cite this article: Mehrjardi NZ, Molcanyi M, Hatay FF, et al. Acquisition of chromosome 1q duplication in parental and genome-edited human-induced pluripotent stem cell-derived neural stem cells results in their higher proliferation rate in vitro and in vivo. *Cell Prolif.* 2020;53:e12892. <https://doi.org/10.1111/cpr.12892>